DOI: 10.1111/mice.13007

RESEARCH ARTICLE

COMPUTER-AIDED CIVIL AND INFRASTRUCTURE ENGINEERING WILEY

Bilevel optimization of a housing allocation and traffic emission problem in a predictive dynamic continuum transportation system

Liangze Yang[1,2] | **S. C. Wong**[3,4] | **H. W. Ho**[5,6] | **Chi-Wang Shu**[7] | **Mengping Zhang**[8]

[1]Yanqi Lake Beijing Institute of Mathematical Sciences and Applications, Beijing, P. R. China

[2]Yau Mathematical Sciences Center, Tsinghua University, Beijing, P. R. China

[3]Department of Civil Engineering, The University of Hong Kong, Hong Kong, P. R. China

[4]Guangdong–Hong Kong–Macau Joint Laboratory for Smart Cities, Institute of Transport Studies. The University of Hong Kong, P. R. China

[5]Department of Civil and Environmental Engineering, The Hong Kong Polytechnic University, Hong Kong, P. R. China

[6]Department of Construction and Quality Management, School of Science and Technology, Hong Kong Metropolitan University, Hong Kong, China

[7]Division of Applied Mathematics, Brown University, Providence, USA

[8]School of Mathematical Sciences, University of Science and Technology of China, Hefei, Anhui, P. R. China

Correspondence
S.C. Wong, Department of Civil Engineering, The University of Hong Kong, Hong Kong, China.
Email: hhecwsc@hku.hk

Funding information
Research Grants Council of the Hong Kong Special Administrative Region, China, Grant/Award Number: 17208614; Guangdong Science and Technology Department, Grant/Award Number: 2020B1212030009; NSF, Grant/Award Number: DMS-2010107; NSFC, Grant/Award Number: 11471305

Abstract

In recent decades, the effects of vehicle emissions on urban environments have raised increasing concerns, and it has been recognized that vehicle emissions affect peoples' choice of housing location. Additionally, housing allocation patterns determine people's travel behavior and thus affect vehicle emissions. This study considers the housing allocation problem by incorporating vehicle emissions in a city with a single central business district (CBD) into a bilevel optimization model. In the lower level subprogram, under a fixed housing allocation, a predictive dynamic continuum user-optimal (PDUO-C) model with a combined departure time and route choice is used to study the city's traffic flow. In the upper level subprogram, the health cost is defined and minimized to identify the optimal allocation of additional housing units to update the housing allocation. A simulated annealing algorithm is used to solve the housing allocation problem. The results show that the distribution of additional housing locations is dependent on the distance and direction from the CBD. Sensitivity analyses demonstrate the influences of various factors (e.g., budget and cost of housing supply) on the optimized health cost and travel demand pattern.

1 | INTRODUCTION

Air pollution has become one of the most important problems in today's world, with serious effects on ecosystems, economies, and human health. Transportation has been identified as a major man-made contributor to air pollutant emissions, and one study determined that approximately 45% of all air pollution emitted in the United States is produced directly by vehicle emissions (Soffer et al., 1995). Vehicle emissions contain very high concentrations of NO_x (Chen & Liu, 2010; Tong et al., 2000), and motor vehicles contribute approximately 35% of all emissions of this pollutant (Nizich et al., 1994). Despite the use of advanced vehicle technologies, such as electric motors, to reduce fuel consumption and traffic-related emissions, two problems remain: First, there is no guarantee that in the future, all vehicles will be electric. If some vehicles still use fossil fuels, emissions will remain a problem. Second, even if possible, the transformation to 100% electric vehicles may take decades. Emissions during this transition period thus need to be considered. Transportation and/or land-use design/policies, such as land-use changes, housing allocation, and emission permits, have been identified as promising approaches for addressing traffic-related air pollution by changing travel behaviors within cities (Barthelemy, 2016; Nagurney et al., 1998).

It is well known that interaction between land use and transportation is bidirectional. On one hand, land use defines the travel demands within a city and the corresponding travel patterns and disutilities as these demands are applied to the transportation system. On the other hand, the resulting travel patterns and disutilities will in turn affect future land-use designs. This reciprocal relationship was first demonstrated in Washington, D.C. (Hansen, 1959) and has since been accepted worldwide and used as the basis for many transportation and land-use models (Giuliano, 1989, Lin et al., 2021, Yin et al., 2017). Of these, the model proposed by Lowry (1964) was most influential, as it was the first analytical tool to consider the land-use and transportation feedback cycle. Subsequently, many models have been established in recent decades and can be classified into following four groups: spatial interaction, mathematical programming, random utility, and bid-rent models (Chang & Mackett, 2006). However, few studies of land-use and transportation models have considered environmental aspects, such as noise pollution and vehicle emissions. Environmental factors (e.g., vehicle emission) were shown to affect land-use and travel patterns, and therefore these factors must be included when modeling the interactions between land use and transportation (Wegener, 2004). Wagner and Wegener (2007) introduced the interactions between land-use, transportation, and environment models in detail, and several models have been established, including the Urbanism model (Wadell, 1998), MEPLAN model (Echenique, 1985), and PECAS model (Hunt & Abraham, 2005).

Land-use patterns, which explore where people live, work, shop, and entertain, influence the travel patterns and evolution of transportation infrastructure. The choice of housing location is fundamental to a land-use model and is traditionally considered to represent a trade-off between the costs of housing rent and transportation (Giuliano, 1989). Wheaton (1977) found that a decision to live further from a city center requires an income elasticity of land consumption that exceeds the income elasticity of the travel cost (including the value of commuting time). Although that study was able to solve the housing location choice model analytically, its various assumptions that simplified the theory (e.g., assumption of a monocentric model) have been criticized. To overcome these simplifying assumptions, several housing location choice models based on the trade-off between land rent and transportation costs have been developed for polycentric cities (Hartwick & Hartwick, 1974; Ogawa & Fujita, 1980). Rosen (1974) describes the relationship between providers and buyers by proposing the hedonic theory, and this theory is now widely used to describe housing rent. However, Ellickson (1981) suggested that hedonic prices are not sufficient to describe travelers' behavior. To better model this behavior, recent studies have adopted the random utility theory (e.g., the logit model) when modeling the housing location choice (Ben-Akiva & Bowman, 1998; Bhat & Guo, 2004; Zondag & Pieters, 2005). Various types of factors influencing houses and households have been considered, such as the house sizes and neighborhood environments, family structures, distances from schools, and networks (Schirmer et al., 2014) in the utility function used to determine housing location choices.

In a housing location choice model, travel cost is one of the most important determinants of the housing location. This cost is a measure of the transportation network performance and has been widely studied and analyzed in the context of transportation network and city planning and management. Wardrop (1952) first used the concept of supply and demand equilibrium in economics to the transportation problem, and the traffic equilibrium problems have since received much attention in recent decades. Generally, there are two main modeling approaches in these studies: discrete modeling or continuum modeling. The first involves a conventional traffic equilibrium model that has been adapted for a detailed transportation problem. In this approach, travel demands are concentrated at zone centroids and connected to road links, which are modeled separately (Lee & Boyces, 2004). In contrast, the latter assumes that the transportation system is very dense. Thus, the characteristics, or transportation variables (e.g., traffic density, travel demand, and local travel cost), are assumed to be continuous and can be described

using smooth mathematical functions (Vaughan, 1987). These two modeling approaches have also been explored extensively in the literature and applied to various types of problems. The discrete modeling approach is more suitable for detailed transportation network management and analysis problems. For example, Bell et al. (1999) applied the discrete modeling approach to a road network reliability analysis, and Yin and Lawphongpanich (2006) and Nagurney et al. (2010) used this approach to study the relationship between a road network and traffic emissions. The continuum modeling approach has the following benefits over the discrete modeling approach (Blumenfeld, 1977; Du et al., 2013; Ho & Wong, 2007). First, the continuum modeling approach reduces the problem size when modeling a dense transportation network because it approximates the region as a continuum instead of modeling each of the links/nodes. Second, because it is not necessary to define each link/node in the modeled region, the continuum approach requires less data for model building and is more suitable for initial-stage planning, when data availability is typically limited. This approach therefore has advantages when addressing housing allocation problems in city planning. Third, because no links or nodes are considered, the continuum modeling approach places a greater focus on the trends and patterns that lead to a better understanding of various global characteristics of the modeling region, such as travel demand, land development intensity, and travel cost.

Today, traffic-related emissions are of particular concern (International-Energy-Agency, 2006) with respect to the various adverse impacts of traffic on the environment (e.g., vehicle emissions and noise pollution; Rodrigue et al., 2016). In the literature, both macro- and microscale approaches to traffic emission problems have been described (Nejadkoorki et al., 2008). Generally, a macroscale approach is used to consider an emission problem affecting a large area (e.g., city or country) for a long period of time (e.g., 1 year or season). This type of approach generally includes averaged and aggregated parameters. Well-known models based on a macroscale approach are MOBILE (EPA, 1994) and EMFAC (CARB, 2006). Compared with the microscale approach, the macro-scale approach needs less computational cost but is inaccurate. In contrast, the microscale approach uses vehicle engine or vehicle speed/acceleration data to estimate the vehicle emissions rate. Some well-known models based on the microscale approach are the VT-Micro (Ahn et al., 1999), VERSIT (Smit et al., 2007), and motor vehicle emission simulator (MOVES) models (Vallamsundar & Lin, 2011).

In addition to emissions, the dispersion of air and atmospheric pollutants (e.g., NO_x and CO_2) should also be considered to ensure an accurate evaluation of the concentrations of these pollutants over the region of interest (e.g., city). The dispersion of air pollution near the Earth's surface is affected by turbulent eddy motion of the wind. Accordingly, the concentration of a pollutant can be determined by using an advection–diffusion equation. Many different dispersion models have been derived (Ermak, 1977; Stockie, 2011). The Gaussian dispersion model (Hickman & Colwill, 1982; Stockie, 2011) is used extensively to simulate the dispersion of air pollution over local and urban areas and can be subclassified as a Gaussian plume dispersion (Loos et al., 2003; Turner & Hurst, 2001) or Gaussian puff dispersion (Fallah-Shorshani et al., 2017; Hargreaves & Baker, 1997). A Gaussian plume dispersion describes a source that continuously emits a contaminant, whereas a Gaussian puff dispersion refers to a nearly instantaneous emission of a contaminant (i.e., occurring over a relatively short time interval). The Gaussian dispersion model (Yin et al., 2017) and a three-dimensional advection–diffusion equation (Yang et al., 2019) have been used recently to model air pollutant concentrations more realistically.

Governments have introduced housing allocation policies to manage air emissions from vehicles and reduce health cost. Although governments make policies, the effectiveness of the policies depends on the actions of the citizens, who choose their housing locations and influence the traffic demand. Given this characteristic, bilevel optimization models have been widely adopted to study these types of problem, such as housing allocation (Boyce & Mattsson, 1999; Lin et al., 2021; Yin et al., 2017), highway road pricing (labbé et al., 1998), and ship air emissions (Qi et al., 2021). In these bilevel models, the lower level subprogram is a traffic equilibrium problem that provides the network conditions (e.g., travel time) to the upper level subprogram, which addresses the housing allocation, such that the planning objectives are optimized (e.g., total disutility of travelers is minimized). Boyce and Mattsson (1999) were among the first researchers to use a bilevel model to study the connection between housing location and traffic based on a discrete modeling approach. Yin et al. (2013) updated this bilevel model by incorporating the environmental factor. However, all of the above studies only addressed static problems and did not consider temporal variations in various parameters (e.g., demand, travel time) in their solutions of integrated land-use, transportation, and environment problems (Yin et al., 2013, 2017).

In this paper, a bilevel model is used to consider a housing allocation problem. In the lower level subprogram, the housing decision (i.e., housing location choice) and travel choices (i.e., departure time and route choices) are determined based on a given housing allocation, for which a predictive dynamic continuum user-optimal (PDUO-C) model (Du et al., 2013) is used to describe traffic flow. The housing location choices of travelers is assumed to depend

on housing rent costs, traffic-related costs, and air quality, the latter of which is affected only by traffic emissions. In traffic analysis, not all of the analyzed quantities can be reasonably defined in links and nodes, which is a requirement of the discrete modeling approach. For example, although air pollutants are emitted by vehicles traveling on roads/links, the dispersion of these air pollutants is continuous over the residential and commercial areas of an entire city (Stockie, 2011). Continuum models can directly and precisely estimate continuously varying quantities (e.g., the concentration of air pollutants) and incorporate them into the analysis. Fixed sources of emissions is considered in Yang et al. (2022), in which a plant located at the margin of the city has a strong effect on the nearby location, especially downwind of the plant, because the emission rate of the plant is much higher than that of vehicles. At the upper level, the health cost is minimized (Yang et al., 2022) by choosing the optimal additional housing allocation and updating the housing allocation accordingly.

Traffic emission is recognized as one of the key concerns of the transportation industry. The interaction between land use and transportation is bidirectional, and housing location choice is a fundamental aspect of land use. Thus, housing allocation patterns define travel demand and related travel patterns and determine vehicle emissions. In addition, air quality influences housing location choice. Owing to its importance and usefulness, a housing allocation problem incorporating air quality has long been a primary concern of researchers, planners, and decision makers (Barthelemy, 2016). This study considers a housing allocation problem by incorporating vehicle emissions in a city with a single central business district (CBD) into a bilevel model and examining the connection between housing allocation and traffic emissions. The housing allocation model devised in the current study is based on the dispersion model of air pollutants devised by Yang et al. (2019) and the housing location choice model developed by Yang et al. (2022). Our aim is to establish an integrated land-use, transportation, and environment model to provide an evaluation/design tool for planners. This study makes the following two contributions. First, a bilevel predictive dynamic continuum transportation model is used to consider a housing allocation problem in which the health cost is defined in terms of the effects of vehicle emissions and set as the optimal objective in an upper level subprogram. This is different from the traditional optimal objective to minimize the total amount of emissions. Second, a predictive traffic model to describe commuter activity in the housing allocation problem is used. As commuters travel to the CBD each day and are very familiar with local transportation, they have perfect information about transportation and the predictive model is suitable for studying city commuter activity in a housing allocation model.

This paper is organized as follows. Section 2 gives the formulation of the bilevel dynamic continuum model. Section 3 introduces the solution algorithms. Section 4 uses a numerical example to demonstrate the characteristics of the model and the effectiveness of the solution algorithm. Finally, Section 5 presents our conclusions.

2 | MODEL FORMULATION

To facilitate the presentation of essential ideas, the following assumptions are adopted in this paper:

- A1 The proposed model falls within the category of continuum modeling approaches for the network equilibrium problem. The road network considered in this study is relatively dense and is approximated as a continuum. Travelers (or vehicles) are free to travel in both the x and y directions within the modeling region (Du et al., 2013; Ho et al., 2006; Yang et al., 2022).
- A2 Travelers have perfect information about traffic conditions (e.g., flows, travel times) over time and are familiar with the modeling region (Du et al., 2013; Yang et al., 2022).
- A3 Only trips from travelers' home locations to the CBD or from the CBD back to their home locations are considered (Yang et al., 2020). Other trips (e.g., trips between the home locations of different travelers) are ignored.
- A4 The modeling period T covers a complete day and is divided into two subperiods: T^1 and T^2. During T^1, all travelers travel from their home locations to CBDs, and no travelers leave the CBDs. During T^2, all travelers travel from CBDs back to their home locations, and no travelers travel to the CBDs (Yang et al., 2019).
- A5 Variations of topography within the modeling region are negligible, and the ground surface (i.e., $z = 0$) can be taken as the plane (Stockie, 2011; Yang et al., 2019).
- A6 Transport-related air pollutants are emitted from a surface source at the ground surface (i.e., $z = 0$; Stockie, 2011; Yang et al., 2019).

A1 and A2 are the basic assumptions for the predictive continuum model. For A3 and A4, as urban commuter activity is the focus in this paper and this activity is dominant in city transportation systems, other travel behavior is ignored. In future studies, multiple travel activities will be considered and these two assumptions are relaxed. A5 and A6 can be relaxed in future studies by considering variations in topography (Britter & Hanna, 2003). Also, different eddy diffusivities $K(\cdot)$ for different land-use characteristics will be considered, such as high-rise building clusters and open spaces.

Consider an urban city with an arbitrary shape and a single CBD (Figure 1) as the modeling region of this study.

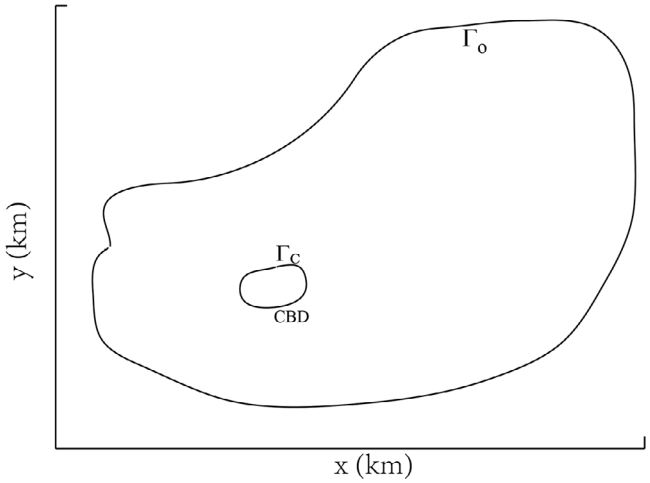

FIGURE 1 An example of a modeling domain. Abbreviations: CBD, central business district.

Let the modeling region be Ω and the outer boundary be Γ_o. The boundary of CBD is denoted by Γ_c. Then, let $\Gamma = \Gamma_o \cup \Gamma_c$ be the boundary of Ω. Note that the domain Ω is a two-dimensional region, but the related boundary Γ is a one-dimensional curve. The travel demand in Ω is assumed to be distributed continuously. All employment and business activities are assumed to occur within the CBD, thus requiring residents to travel back and forth between their home locations and the CBD. Note that travelers will select departure times and route to minimize the costs of this back-and-forth travel.

The flow vector of travelers at location $(x, y) \in \Omega$ and time $t \in T^j$ is defined as $\mathbf{f}(x, y, t) = (f_1(x, y, t), f_2(x, y, t))$, where $f_1(x, y, t)$ and $f_2(x, y, t)$ are the flow-fluxes in the x and y directions, respectively. $T^j = [t^j_{beginning}, t^j_{end}]$ denotes the j-th modeling period. In this study, J denotes the total number of modeling periods, and $J = 2$ (i.e., $j \in \{1, 2\}$). Let $T = T^1 \cup T^2$ represent the complete modeling period, where T^1 and T^2 indicate the modeling periods during which travelers move from their home locations to the CBD and vice versa, respectively. This flow vector is dependent on the density, $\rho(x, y, t)$, and velocity vectors, $\mathbf{v}(x, y, t)$, of the corresponding location (x, y) and time (t), and is defined by the following Equation (1):

$$\mathbf{f}(x, y, t) = \rho(x, y, t)\,\mathbf{v}(x, y, t) \tag{1}$$

Using Equation (1) and the velocity vector $(\mathbf{v}(x, y, t))$, flow intensity (i.e., the norm of the flow vector) is defined as $|\mathbf{f}(x, y, t)| = \rho(x, y, t)V(x, y, t)$. Define $\mathbf{v}(x, y, t) = (v_1(x, y, t), v_2(x, y, t))$ as travelers' velocity vector, where $v_1(x, y, t)$ and $v_2(x, y, t)$ are the velocities in the x and y directions, respectively. Define $V(x, y, t)$ as the speed (in km/h), which is derived by the corresponding velocity vector (i.e., $V(x, y, t) = |\mathbf{v}(x, y, t)|$) and is defined as:

$$V(x, y, t) = V_f(x, y) \exp\left[-\zeta(x, y)\,\rho(x, y, t)\right] \tag{2}$$

where $V_f(x, y)$ is the free-flow speed of the travelers, $\rho(x, y, t)$ is the density, and $\zeta(x, y)$ is positive parameter at location $(x, y) \in \Omega$. The local travel cost, $c(x, y, t)$, satisfies:

$$c(x, y, t) = \frac{\kappa}{V(x, y, t)} + \kappa\pi(\rho(x, y, t)) \tag{3}$$

where κ is value of time. $\frac{\kappa}{V(x,y,t)}$ represents the cost related to travel time. The second term in Equation (3) represents other costs that depend on vehicle density, such as the perceived difficulties of lane-changing and crash risks in a crowded condition with an identical travel time to that represented by the first term. The total travel cost (in \$) $l(x, y, t)$ is defined as:

$$l(x, y, t) = p(x, y, t) + \phi(x, y, t) \tag{4}$$

where $\phi(x, y, t)$ is travel cost potential of the traveler based on the optimal departure time and route choice determined from the lower level subprogram (Section 2.1) to (1) travel from home to the CBD (i.e., going to work) or (2) depart from the CBD to back home (i.e., returning home). Here, p is schedule delay cost. This schedule delay cost is a penalty for an early or late arrival and depends on $t + I(x, y, t)$, where I denotes travel time of travelers from point (x, y) traveling to the CBD (or in the reverse direction). The details of $p(x, y, t)$ will be discussed next. Using the cost potentials at different times, the average transportation cost between location (x, y) and the CBD, $\Phi(x, y, t)$, is defined as:

$$\Phi(x, y) = \frac{1}{|T^2|}\int_{T^2} \phi(x, y, t)\,dt + \frac{1}{|T^1|}\int_{T^1} \phi(x, y, t)\,dt \tag{5}$$

Using the average transportation cost as defined in Equation (5), the total perceived travel cost between location (x, y) and the CBD, $P(x, y)$, is defined as follows:

$$P(x, y) = \theta + S(Q) + \Phi(x, y) \tag{6}$$

where θ represents the travelers' preference for the CBD and $S(Q)$ is the internal operating cost of traffic (e.g., parking cost, local circulation cost) within the CBD and is relied on total travel demand attracted to that CBD, Q, which is defined as:

$$Q = \int_{T^1}\iint_{\Omega} q(x, y, t)\,d\Omega dt \tag{7}$$

Here, $q(x, y, t)$ is travel demand. Based on $q(x, y, t)$, the related total travel demand during modeling period j is defined as $q^j(x, y) = \int_{T^j} q(x, y, t)\mathrm{d}t$. Using the above fundamental definitions, the formulations of the various models applied in this study are introduced in the following subsections.

2.1 | Lower level model

Traffic flow within the modeling region is modeled using the PDUO-C model, which serves as the lower level of the bilevel model in this study. The PDUO-C model is used to explore the combined choices of travelers with respect to housing location, route, and departure time, based on the air quality, perceived travel cost, and housing rent.

2.1.1 | PDUO-C model

This study assumes that travelers are very familiar to the transportation in the city because they commute to the CBD each day. As in Yang et al. (2019), the PDUO-C model can be divided into two periods for modeling the route choices within an entire day. The PDUO-C model of travelers traveling to the CBD ($j = 1$) is defined as follows:

$$\begin{cases} \rho_t + \nabla \cdot \mathbf{f} = q \\ \mathbf{f} = -\rho V \frac{\nabla \phi}{|\nabla \phi|} \\ \mathbf{f}(x,y,t) \cdot \mathbf{n}(x,y) = 0 \qquad \forall (x,y) \in \Gamma \setminus \Gamma_c \\ \rho(x,y,t^1_{beginning}) = \rho_0(x,y)\ \forall (x,y) \in \Omega \end{cases} \tag{8}$$

$$\begin{cases} \frac{1}{V}\phi_t - |\nabla \phi| = -c \\ \phi(x,y,t) = \phi_{CBD} \qquad \forall (x,y) \in \Gamma_c \\ \phi\left(x,y,t^1_{end}\right) = \phi^1_0(x,y)\ \forall (x,y) \in \Omega \end{cases} \tag{9}$$

where $\rho_t = \partial \rho(x,y,t)/\partial t$, $\nabla \cdot \mathbf{f} = (\partial f_1(x,y,t)/\partial x) + (\partial f_2(x,y,t)/\partial y)$, and $\phi_t = \partial \phi / \partial t$; $\mathbf{n}(x,y)$ represent the outer boundary's unit normal vector, and ϕ_{CBD} is value of ϕ on the boundary of the CBD. Based on the analysis in Du et al. (2013), when travel cost ϕ is the integral over the local unit travel cost $c(\cdot)$ and satisfies the Hamilton–Jacobi equation, the travelers traveling along direction $\nabla \phi$ satisfy the predictive dynamic user-optimal condition. This study assumes that the densities will be zero at the start (i.e., $\rho(x,y,t^1_{beginning}) = 0$). Accordingly, ϕ^1_0 can be solved by considering the following 2D Eikonal equation:

$$\begin{cases} \left|\nabla \phi^1_0(x,y)\right| = c\left(x,y,t^1_{end}\right)\ \forall (x,y) \in \Omega \\ \phi^1_0(x,y) = \phi_{CBD} \qquad \forall (x,y) \in \Gamma_c \end{cases} \tag{10}$$

Similarly, model formulation of the second part ($j = 2$) is:

$$\begin{cases} \rho_t + \nabla \cdot \mathbf{f} = q \\ \mathbf{f} = -\rho V \frac{\nabla \phi}{|\nabla \phi|} \\ \mathbf{f}(x,y,t) \cdot \mathbf{n}(x,y) = 0 \qquad \forall (x,y) \in \Gamma \setminus \Gamma_c \\ \rho\left(x,y,t^1_{beginning}\right) = \rho_0(x,y)\ \forall (x,y) \in \Omega \end{cases} \tag{11}$$

$$\begin{cases} \frac{1}{V}\phi_t - |\nabla \phi| = -c \\ \phi(x,y,t) = \phi_{CBD} \qquad \forall (x,y) \in \Gamma_c \\ \phi\left(x,y,t^1_{end}\right) = \phi^1_0(x,y)\ \forall (x,y) \in \Omega \end{cases} \tag{12}$$

Then, ϕ^2_0 can be solved by considering the following 2D Eikonal equation (Equation 13):

$$\begin{cases} \frac{1}{V}\phi_t - |\nabla \phi| = -c \\ \phi(x,y,t) = \phi_{CBD} \qquad \forall (x,y) \in \Gamma_c \\ \phi\left(x,y,t^1_{end}\right) = \phi^1_0(x,y)\ \forall (x,y) \in \Omega \end{cases} \tag{13}$$

2.1.2 | Departure time

Beyond the definition of the travelers' route choice in the last subsection, the travelers' departure time choice is also an important component of a dynamic traffic assignment (DTA) problem. Before introducing the departure time choice model, the schedule delay cost should first be defined. According Du et al. (2013), the travel time $I(x,y)$ satisfies:

$$\frac{1}{V} I_t(x,y,t) - |\nabla I(x,y,t)| = -\frac{1}{V(x,y,t)} \tag{14}$$

Using this travel time, $I(x,y,t)$, the schedule delay cost, $p(x,y,t)$, is defined as follows:

$$p(x,y,t) = \begin{cases} \gamma_1 \left[\left(t^{j*} - \nabla\right) - t_{arv}\right], t_{arv} \in \left[0, t^{j*} - \nabla\right), \\ 0 \qquad\qquad t_{arv} \in \left[t^{j*} - \nabla, t^{j*} + \nabla\right], \\ \gamma_2 \left[t_{arv} - \left(t^{j*} + \nabla\right)\right], t_{arv} \in \left(t^{j*} + \nabla, \infty\right) \end{cases} \tag{15}$$

where $t_{arv} = t + I(x,y,t)$ is actual arrive time that departure from time t, t^{j*} is desired arrival time, ∇, γ_1 and

γ_2 are both positive scalars that define the values of time for early and late arrivals, respectively. According to previous empirical studies (Small, 1982), this study assumes that $\gamma_2 > \kappa > \gamma_1$. Given the above definition of a schedule delay cost, $(p(x,y,t))$, total travel cost, $(l(x,y,t))$, can be calculated using Equation (4).

Given the distribution of the travel demand, q, l can be computed using the PDUO-C model defined in Section 2.1.1. Thus, the total travel cost can be denoted as $l(x,y,t) = l(x,y,t,\mathbf{q}^{\mathbf{j}})$, and the minimum total travel cost of the travelers during modeling period j, $\hat{l}^j(x,y,\mathbf{q}^{\mathbf{j}})$, can be defined as:

$$\hat{l}^j\left(x,y,\mathbf{q}^j\right) = essinf\left\{l\left(x,y,t,\mathbf{q}^j\right), \quad \forall t \in T^j\right\} \tag{16}$$

Similar to Yang et al. (2022), this minimum total travel cost can be used to define the principle for dynamic user-optimal condition with departure-time consideration, as follows:

Definition 1. The dynamic user-optimal condition with departure-time consideration is satisfied during the modeling period, j, if the following equation is satisfied:

$$\begin{cases} l\left(x,y,t,\mathbf{q}^j\right) = \hat{l}^j\left(x,y,\mathbf{q}^j\right), \text{if} q\left(x,y,t\right) > 0 \\ l\left(x,y,t,\mathbf{q}^j\right) \geq \hat{l}^j\left(x,y,\mathbf{q}^j\right), \text{if } q\left(x,y,t\right) = 0 \end{cases} \tag{17}$$

where $\Lambda^j = \{\mathbf{q}^j : q(x,y,t) \geq 0, \int_{T^j} q(x,y,t)\mathrm{dt} = q^j(x,y)\}$ denotes the feasible set of travel demands, $\mathbf{q}^j$.

From Equation (17), the dynamic user-optimal condition ensures that for each traveler departing from the same position at any time, the total travel cost is equal and minimized. In other words, no traveler in the system can reduce their total travel cost by changing their departure time and/or route choice. Based on the above optimality condition, the equivalent variational inequality formulation adopted to solve the departure time and route choice problem is defined by the following theorem.

Theorem 1. The dynamic user-optimal condition in Definition 1 is equivalent to the following variational inequality problem (Equation 18) in modeling period j: Find $\mathbf{q}^{j^*} \in \Lambda^j$ so that for all $\mathbf{q}^j \in \Lambda^j$,

$$\iint_{\Omega}\int_{T^j} l\left(x,y,t,q^{j*}\right)\left(q\left(x,y,t\right) - q^*\left(x,y,t\right)\right)dtd\Omega \geq 0 \tag{18}$$

Detailed proof of the equivalency of this variational inequality problem to the dynamic user-optimal condition with departure-time consideration (Equation 17) is presented in Yang et al. (2022).

2.1.3 | Emission and dispersion model

In this study, the travel cost, housing rent, and air quality in a residential location are assumed to affect the housing location choices of the travelers or residents. The travel cost and housing rent at a location, which are based on the travel demand at that location, can be determined using the above PDUO-C model. The air quality in an urban city is directly affected by traffic-related emissions. In the literature, most of the developed vehicle emission models were established at a microscopic level (i.e., individual vehicles) and depend on the instantaneous vehicular speed and acceleration (Ahn et al., 1999; Yang et al., 2019). These models cannot be applied directly in this study, as the PDUO-C model is formulated at the macroscopic level. Thus, the macroscopic emission model proposed in Yang et al. (2022) is adopted to determine the traffic-related emissions in this study (Equation 19).

$$\Psi(x,y,t) = \psi(V,a) + \frac{1}{2}\frac{\partial^2\psi(V,a)}{\partial(U)^2}(\sigma_V)^2 + \frac{1}{2}\frac{\partial^2\psi(V,a)}{\partial(s)^2}(\sigma_a)^2 \tag{19}$$

where $\Psi(x,y,t)$ is macroscopic emission rate that describes average emission rate. $V = V(x,y,t)$ and $a = a(x,y,t)$ ($\sigma_V = \sigma_V(x,y,t)$ and $\sigma_a(x,y,t)$) are the mean (standard deviation) of the instantaneous speed $(U = U(x,y,t))$ and instantaneous acceleration $(s = s(x,y,t))$, respectively. According to Yang et al. (2020), $U(x,y,t)$ and $s(x,y,t)$ are random variables that follow certain normal distributions (i.e., $U(x,y,t) \sim N(V(x,y,t),\sigma_V)$ and $s(x,y,t) \sim N(a(x,y,t),\sigma_a)$). The macroscopic emission model (Equation 19) is then derived by applying the Taylor expansion of the microscopic emission model in Ahn et al. (1999) (Equation 20) up to second-order terms (Yang et al., 2020)

$$\psi(x,y,t) = \psi\left(U\left(x,y,t\right), s\left(x,y,t\right)\right) = \exp\left[\sum_{i=0}^{3}\sum_{k=0}^{3} w_{i,k}[U\left(x,y,t\right)]^i[s\left(x,y,t\right)]^k\right] \tag{20}$$

where $\omega_{i,k}$ is model regression coefficient. This value differs for various types of emissions (e.g., hydrocarbons, CO,

or NO_x), which are given by Ahn et al. (1999) and Yang et al. (2022). The emission rate is dependent on the vehicle speed and acceleration, which are affected by the level of traffic congestion. Thus, traffic congestion affects both delays (i.e., travelers' loss of time) and levels of emissions (i.e., health impacts on travelers/residents). In summary, $U(x,y,t)$, $s(x,y,t)$, and $\psi(x,y,t)$ are defined at a microscopic level (i.e., for a single vehicle), whereas $V(x,y,t)$, $a(x,y,t)$, and $\Psi(x,y,t)$ are defined at the macroscopic level when individual vehicles (based on the macroscopic model) cannot be distinguished. The instantaneous acceleration ($a(x,y,t)$) for travelers along their PDUO-C route satisfy (Yang et al., 2022):

$$a(x,y,t) = \frac{a_1(x,y,t)\,\phi_x(x,y,t) + a_2(x,y,t)\,\phi_y(x,y,t)}{\sqrt{\left[\phi_x(x,y,t)\right]^2 + \left[\phi_y(x,y,t)\right]^2}} \tag{21}$$

where $a_1(x,y,t)$ and $a_2(x,y,t)$ represent the accelerations in the x and y directions, respectively, at location (x,y) and time t, $\phi_x(x,y,t) = \partial\phi(x,y,t)/\partial x$ and $\phi_y(x,y,t) = \partial\phi(x,y,t)/\partial y$. $a_1(x,y,t)$ and $a_2(x,y,t)$ are further defined as:

$$a_1(x,y,t) = \frac{\partial v_1(x,y,t)}{\partial t} + v_1(x,y,t)\frac{\partial v_1(x,y,t)}{\partial x} + v_2(x,y,t)\frac{\partial v_1(x,y,t)}{\partial y} \tag{22}$$

$$a_2(x,y,t) = \frac{\partial v_2(x,y,t)}{\partial t} + v_1(x,y,t)\frac{\partial v_2(x,y,t)}{\partial x} + v_2(x,y,t)\frac{\partial v_2(x,y,t)}{\partial y} \tag{23}$$

This study assumes that the vehicle exhaust will disperse via turbulent diffusion and wind advection, and therefore the exhaust concentration satisfies the below equation:

$$\frac{\partial C(\cdot)}{\partial t} + \nabla\cdot\left(C(\cdot)\,u_f(\cdot)\right) = \frac{\partial}{\partial x}\left(K_x\frac{\partial C(\cdot)}{\partial x}\right) + \frac{\partial}{\partial y}\left(K_y\frac{\partial C(\cdot)}{\partial y}\right) + \frac{\partial}{\partial z}\left(K_z\frac{\partial C(\cdot)}{\partial z}\right) + \hat{S}(\cdot) \tag{24}$$

where $C(\cdot) = C(x,y,z,t)$ is the air pollutant concentration at location (x,y,z) and time t, $\mathbf{u}_f = \mathbf{u}_f(x,y,z,t)$ represents vector of wind velocity; and K_x, K_y, and K_z represent the eddy diffusivities, $\hat{S}(\cdot) = \hat{S}(x,y,z,t) = \hat{S}_0(x,y,z,t) + \hat{S}_t(x,y,z,t)$ (in kg/km^{3}h) is the source term used to define the source of air pollutants (i.e., $C(x,y,z,t)$) at location (x,y,z) at time t, where $\hat{S}_t(x,y,z,t)$ represents the air pollutants from traffic and $\hat{S}_0(x,y,z,t)$ represents the air pollutants from other sources (e.g., power plants, residents' activities). The source terms are

$$\hat{S}_t(x,y,z,t) = \delta(z)\,\rho(x,y,t)\,\Psi(x,y,t) \tag{25}$$

$$\hat{S}_0(x,y,z,t) = \delta(z)\,\varrho(x,y,t) \tag{26}$$

where $\delta(z)$ (in km^{-1}) is the Dirac delta function, and $\varrho(x,y,t)$ represents emission rate of the other sources, and $\Psi(x,y,t)$ is the emission rate of vehicles at a macroscopic level.

2.1.4 | Housing location choice

In the above section, the total travel demand $q(x,y)$ is always given, where pass superscript j for simplicity. This term is now defined in this subsection. This paper assumes that travelers choose their housing location according to the total travel cost, housing rent, and air quality distribution in the city. The housing allocation problem is incorporated into the transportation equilibrium problem by the following equation:

$$q(x,y) = Q\frac{exp\left(-\hat{\gamma}\sigma(x,y)\right)}{\iint_\Omega exp\left(-\hat{\gamma}\sigma(x,y)\right)d\Omega} \tag{27}$$

where Q is total travel demand in modeling region Ω, $\sigma(x,y)$ is housing utility function, and $\hat{\gamma}$ is a positive scalar parameter. Similar to Yang et al. (2022), the housing utility function, $\sigma(x,y)$, which depends on total travel cost, housing rent, and air quality, is satisfied:

$$\sigma(x,y) = P(x,y) + \tau(x,y) + r(x,y) \tag{28}$$

where $P(x,y)$ is the the total perceived travel cost as defined in Equation (6). $\tau(x,y)$ represents travelers' perception of air quality, which is assumed to share a linear relationship with the average local pollutant concentration ($\bar{C}(x,y,0)$, and is defined by:

$$\tau(x,y) = \xi\bar{C}(x,y,0) \tag{29}$$

where ξ represents the sensitivity of the travelers to the air quality, and $\bar{C}(x,y,0) = \frac{1}{|T|}\int_T C(x,y,0,t)\mathrm{d}t$ is the average local pollutant concentration at ground level. $r(x,y)$ is housing rent, and is defined by:

$$r(x,y) = \alpha(x,y)\left(1 + \frac{\beta(x,y)\,q(x,y)}{H(x,y) - q(x,y)}\right) \tag{30}$$

where $\alpha(x,y)$ and $\beta(x,y)$ is a scalar parameter, H is total housing-supply density. This latter variable satisfies:

$$H(x,y) = h_0(x,y) + h(x,y) \tag{31}$$

where $h_0(x,y)$ is the existing housing provision density. Note that $H(x,y)$ at any location (x,y) should be greater than q.

In addition to housing location choice, the travel demand, $(q(x,y,t))$, is also dependent upon departure time choice and can be written as $q(x,y,t) = q(x,y)g(x,y,t)$, where $g(x,y,t)$ is departure-time distribution during period j and $\iint_{T_j} g(x,y,t)dt = 1$. In departure time choice model, $q(x,y)$ is fixed to determine a $g(x,y,t)$, or $q(x,y,t)$ that satisfies the dynamic user-optimal condition with departure-time consideration. In contrast, this section aims to find a desired $q(x,y)$ for a fixed $g(x,y,t)$.

2.2 | Upper level subprogram

In the lower level subprogram, based on the housing allocation $H(x,y)$ obtained from the upper level subprogram, the housing decision (i.e., housing location choice) and travel choice (i.e., departure time and route choice) of travelers are solved. In the upper level subprogram, based on the housing location choice, the housing allocation is updated by the additional housing allocation, and the optimal additional housing allocation is determined by minimizing the overall health cost Y (Yang et al., 2022) of the modeling region, which is defined as follows:

$$\mathrm{Y} = \iint_{\Omega} (x,y,0)\, q(x,y)\, d\Omega \tag{32}$$

Using the above definition of (Y), the upper level subprogram can be written as the following optimal problem:

$$\min_{h(x,y)} \mathrm{Y}(h(x,y)) = \iint_{\Omega} \bar{C}(x,y,0)\, q(x,y)\, d\Omega \tag{33}$$

subject to

$$\begin{cases} h_{\max}(x,y) - h(x,y) \geq 0, \quad \forall (x,y) \in \Omega \\ h(x,y) \geq 0, \quad \forall (x,y) \in \Omega \\ B - \iint_{\Omega} P(x,y)\, h(x,y)\, d\Omega \geq 0 \\ h(x,y) + h_0(x,y) - q(x,y) \geq 0 \end{cases} \tag{34}$$

where $h_{\max}(x,y)$ is maximum additional housing supply density. B is total budget and $G(x,y)$ is unit cost for housing supply. The first inequality constraint in Equation (34) ensures that the additional housing supply density is always less than maximum additional housing supply density. The second inequality constraint in Equation (34) ensures that the housing supply will not be reduced. The third inequality constraint in Equation (34) ensures that the additional housing supply provision cost cannot exceed the total budget. The last inequality constraint in Equation (34) is a natural constraint to ensure a sufficient housing supply for all travel demands at location (x,y).

3 | SOLUTION ALGORITHM

3.1 | Solution algorithm for the lower level subprogram

For the lower level subprogram introduced in Section 2.1, this study adopts the Lax–Friedrichs scheme to solve the conservation law equation (Equations 8 and 11) and the Hamilton–Jacobi equation (Equations 9 and 12) in the PDUO-C model. Moreover, the fast-sweeping method is adopted to solve the Eikonal equation (Equation 10 and Equation 13). Details about the use of these algorithms can be found in Yang et al. (2022).

3.2 | Solution algorithm for the upper level subprogram

According to the description of the upper level subprogram in Section 2.2, the upper level model equivalent a constrained optimization problem about optimal variable $h(x,y)$. To derive a realistic and reliable solution for this upper level subprogram, a finer grid, in which the additional housing provision $h(x,y)$ is defined at each grid point, should be considered. However, such a fine grid would lead to a large problem size because the number of variables depends on the number of grid points. This would substantially increase the computation cost. Additionally, as the macroscopic and continuum model has been applied to model the traffic flows and exhaust emission and dispersion, it is reasonable to define the housing provision at the macroscopic level.

Accordingly, this paper assumes that $h(x,y)$ is a function dependent on the distance and direction from the CBD defined as:

$$h(x,y) = \sum_{m=1}^{M} d^m(x,y) \left(\sum_{n=0}^{N} (a_{m,n} \sin(j\theta(x,y)) + b_{m,n} \cos(j\theta(x,y)) \right) \tag{35}$$

where $d(x,y)$ and $\theta(x,y)$ are the distance and direction about the center of the CBD, respectively, and $\theta(x,y)$ is counterclockwise start from positive x-axis. The additional housing provision is a continuous function and thus can be constructed based on the Fourier series. In a mathematical method, the Fourier series provides a good approximation of a continuous function if indexes M and N are sufficiently large. Based on this approximation, the optimal variables can be reduced to $2MN+1$. By substituting Equation (35) into Equations (33) and (34), the constrained optimization problem can be updated as follows:

$$\min_{h(x,y)} \Upsilon\left(h\left(x,y\right)\right) = \iint_{\Omega} \bar{C}\left(x,y,0\right) q\left(x,y\right) d\Omega \tag{36}$$

subject to

$$\begin{cases} \begin{cases} h_{\max}\left(x,y\right) - \sum_{m=1}^{M}\sum_{n=0}^{N} a_{m,n} d^{m}\left(x,y\right) \sin\left(n\theta\left(x,y\right)\right) - \\ \quad \sum_{m=1}^{M}\sum_{n=0}^{N} b_{m,n} d^{n}\left(x,y\right) \cos\left(n\theta\left(x,y\right)\right) \geq 0, \end{cases} \\ \begin{cases} \sum_{m=1}^{M}\sum_{n=0}^{N} a_{m,n} d^{m}\left(x,y\right) \sin\left(n\theta\left(x,y\right)\right) + \\ \sum_{m=1}^{M}\sum_{n=0}^{N} b_{m,n} d^{m}\left(x,y\right) \cos\left(n\theta\left(x,y\right)\right) \geq 0, \end{cases} \\ \begin{cases} B - \iint_{\Omega} P\left(x,y\right) \left(\sum_{m=1}^{M}\sum_{n=0}^{N} a_{m,n} d^{m}\left(x,y\right) \sin\left(n\theta\left(x,y\right)\right) + \right. \\ \quad \left. \sum_{m=1}^{M}\sum_{n=0}^{N} b_{m,n} d^{m}\left(x,y\right) \cos\left(n\theta\left(x,y\right)\right) \right) d\Omega \geq 0 \end{cases} \\ \begin{cases} \sum_{m=1}^{M}\sum_{n=0}^{N} a_{m,n} d^{m}\left(x,y\right) \sin\left(n\theta\left(x,y\right)\right) + \\ \sum_{m=1}^{M}\sum_{n=0}^{N} b_{m,n} d^{m}\left(x,y\right) \cos\left(n\theta\left(x,y\right)\right) + h_{0}\left(x,y\right) - q\left(x,y\right) \geq 0 \end{cases} \end{cases} \tag{37}$$

where $h(x,y)$ depends on $a_{m,n}, b_{m,n}$ as calculated using Equation (35); thus, the optimal variables are $a_{m,n}, b_{m,n}$. Next, a solution algorithm is developed to solve the above minimization problem. As shown by the objective function (Equation 36), the design variable, that is, additional housing provision $h(x,y)$, is not included. In fact, the objective function Y implicitly couples the design variable $(h(x,y))$ with the average air pollutant concentration $(\bar{C}(x,y,0))$ and the travel demand $(q(x,y))$, as these two variables are solved in the lower level subprogram that depends on $h(x,y)$. Therefore, this is an implicitly optimal problem that is difficult to solve using traditional optimization theories such as the gradient descent method, Newton's method, and the conjugate gradient method because most of these methods require the gradient of the objective function. However, as the objective function in our study is in an implicit form, it is difficult to mathematically derive its gradient. Although the gradient can be computed numerically, the corresponding computational cost for a fine grid will be very high. Therefore, simulated annealing (SA) is proposed to solve the upper level subprogram.

The SA algorithm, which was first introduced by Metropolis et al. (1953), is among the most popular heuristic algorithms. Subsequently, according to the similarity between the solid matter annealing process in physics and general combinatorial optimization problems, Kirkpatrick et al. (1983) successfully introduced the concept of annealing to the field of combinatorial optimization. In fact, this algorithm is a general stochastic optimization algorithm based on a Monte Carlo iterative solution strategy. Thus, SA is a probabilistic technique for approximating the global optimum of a given function. This technique can be used for very complex computational optimization problems for which exact algorithms fail. Although it can usually only achieve an approximate solution to the global minimum, it is sufficient for many practical problems. It has been used widely in engineering applications such as very large-scale integration (VLSI), production scheduling, control engineering, machine learning, neural networks, and signal processing. The procedure of the SA algorithm is as follows:

1. Given an initial temperature T, the maximum iteration number k_{max}, and the ending temperature T_0.
2. Set $k=1$, assume an initial additional housing allocation h_k, and compute the health cost Υ_k.
3. Choose a new additional housing allocation, h', randomly in the neighborhood of h_k, and compute the related health cost Υ'.
4. Compute $\Delta\Upsilon = \Upsilon' - \Upsilon_k$. if $\Delta\Upsilon < 0$, then set $h_{k+1} = h'$ and $\Upsilon_{k+1} = \Upsilon'$; otherwise, compute $P_k = \frac{1}{1+e^{-\Delta\Upsilon/T}}$, and choose a random number Pr in the interval (0,1). If $Pr < P_k$, then set $h_{k+1} = h'$ and $\Upsilon_{k+1} = \Upsilon'$; otherwise, $h_{k+1} = h_k$ and $\Upsilon_{k+1} = \Upsilon_k$.
5. If $k \geq k_{max}$, go to Step 6; otherwise, set $k = k+1$. Go to Step 3.
6. If $T < T_0$, stop; otherwise, set $T = oT$, then go to Step 2.

4 | NUMERICAL EXPERIMENTS

In Figure 2, a modeling region (length, 35 km; width, 25 km) with a single CBD is considered. The center of this compact CBD (area, 2 km × 2 km) is located at (6 km, 10 km). This study considers vehicular travel to and from the CBD during a complete day. For simplicity, it is assumed that vehicles travel to the CBD in the morning and back to the travelers' homes in the evening.

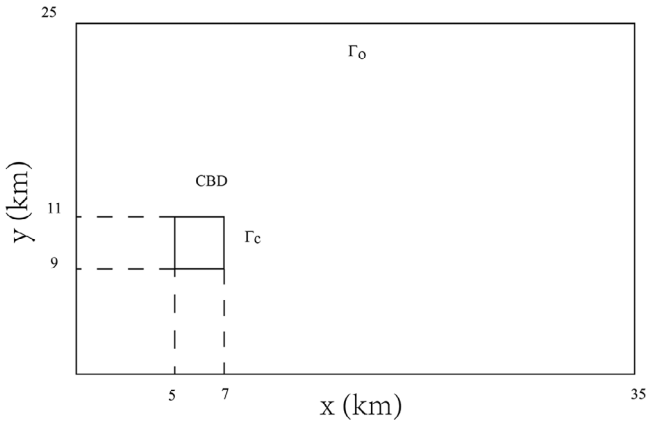

FIGURE 2 The rectangular modeling region. Abbreviations: CBD, central business district.

Other travel behaviors are ignored. The dispersion of vehicle exhaust is modeled in the 3D space $\Omega \times [0, 1]$.

This numerical experiment assumes a lack of travelers at the beginning and a cost of zero to enter or leave the CBD (i.e., $\rho(x, y, 0) = 0$, and $\phi_{CBD} = 0$). This paper considers traffic flow and the related vehicle exhaust's dispersion within the modeling domain from 6:00 a.m. on the first day to 6:00 a.m. on the following day. Thus, the modeling period is $T = [0, 24\,\text{h}]$, with the first subperiod ranging from 6:00 a.m. to 5:00 p.m. (i.e., $T^1 = [0, 11\,\text{h}]$) and the second from 5:00 p.m. to 6:00 a.m. on the following day (i.e., $T^2 = [11, 24\,\text{h}]$). In the speed function (Equation 2), the free-flow speed, V_f, is given by the following function:

$$V_f(x, y) = V_{\max}[1 + \gamma_3 d(x, y)] \tag{38}$$

where $V_{\max} = 56\,\text{km/h}$ and $\gamma_3 = 4 \times 10^{-3}\text{km}^{-1}$. In this numerical example, the standard deviation of speed and acceleration are both set at 0.2 (i.e., $\sigma_V = \sigma_a = 0.2$), and the local travel cost function is set at $c(x, y) = 90(\frac{1}{V} + 10^{-8}\rho^2)$. When considering travelers to or from the CBD, this study assumes that all travelers have the same desired arrival time as they travel to or return from the CBD. Therefore, this numerical example defines the desired arrival (period 1) and departure times (period 2) as $\{t^{1^*}, t^{2^*}\} = \{2.8\text{h}, 12.5\,\text{h}\}$. In the schedule-delay cost function (Equation 15), the parameters γ_1, γ_2, and ∇ are set at 48 \$/h, 108 \$/h, and 0.2 h, respectively. The total perceived CBD cost (Equation 6) comprises biased, demand-related, and travel cost components. The biased cost is a constant, $\theta = 12$, and the demand-related cost is defined as $S(Q) = 8 \times 10^{-11}(Q - 100,000)^2$, where Q is the total travel demand in the whole city and is set at 200,000. The other emission rate is taken as $\varrho(x, y, t) = (L(t))/Q(\text{kg}/(\text{km}^2\text{h}))$ in the CBD; here, $L(t)$ denotes the cumulative number of vehicles in the CBD at time t.

In this numerical example, the convergence threshold for the lower level subprogram is set at $\varepsilon_1 = 0.005, \varepsilon_2 = 10^{-9}$, and $\varepsilon = 0.01$ (see Yang et al., 2022). The dispersion of pollutants is modeled within the 1 km space over the rectangular modeling region (i.e., $\hat{\Omega} = [0, 35] \times [0, 25] \times [0, 1]$). The model assumes that the wind velocity $\mathbf{u}_f(x, y, z, t) = (10, 0, 0)$ and eddy diffusivity are both $0.01\,\text{km}^2/\text{h}$ (i.e., $K_x = K_y = K_z = 0.01$). The travelers' sensitivity to the housing utility ($\hat{\gamma}$) and air quality (ξ) are set at 0.0015 and 10, respectively. For the housing rent function, $r(x, y)$, the related parameters $\alpha(x, y))$ and $\beta(x, y)$ are, respectively, set at 5 and 8. The existing housing provision, $h_0(x, y)$, is set at 300 unit/km^2 and the maximum housing supply, $h_{\max}$, is taken as 350 unit/km^2. The budget, B, is set at 1 billion dollars. Accordingly, the cost for the unit housing supply, $G(x, y)$, is defined by

$$G(x, y) = G_0\left(1 + \frac{0.01}{\sqrt{(x-6)^2 + (y-10)^2}}\right) \tag{39}$$

where the basic cost $G_0 = 10000$. In this numerical example, the settings in Equation (35) are $M = 3, N = 1$. In the SA algorithm, the initial temperature $T = 350$, ending temperature $T_0 = 10$, maximum iteration number $k_{\max} = 50$, and frozen coefficient $o = 0.9$. In our model, the housing location choices are determined by the lower level model, travel costs, and flow patterns under a fixed housing allocation. The self-adaptive method of successive averages (MSA) (Du et al., 2013) is used to solve a lower level subprogram, of which a detailed discussion can be found in Yang et al. (2022).

Two grids (Grid 1: $35 \times 25 \times 50$; Grid 2: $70 \times 50 \times 100$) are tested to consider convergence. The computational time is approximately 36 h for the first grid and approximately 240 h for the second. In this paper, the number of iterations is more than 1500, and the frozen coefficient is taken as 0.9. The initial temperature is set as 350, and at each temperature, the maximum iteration is set as 50. It is believed that these parameters are sufficient to derive the desired solution.

In this study, a conventional genetic algorithm (GA) is also adopted to solve this bilevel problem, to provide a comparison with the performance of our SA algorithm. Figure 3 shows the convergence curves of the SA algorithm and those for GA1 and GA2. The latter are two forms of GA; in GA1, the initial solution set is randomly chosen, whereas in GA2, the initial solution set is chosen such that it is close to the optimal solution obtained by the SA algorithm. It can be seen that the convergence rate of the GA is much slower than that of the SA algorithm, especially when the initial solution is randomly chosen (i.e., for GA1). Over a given

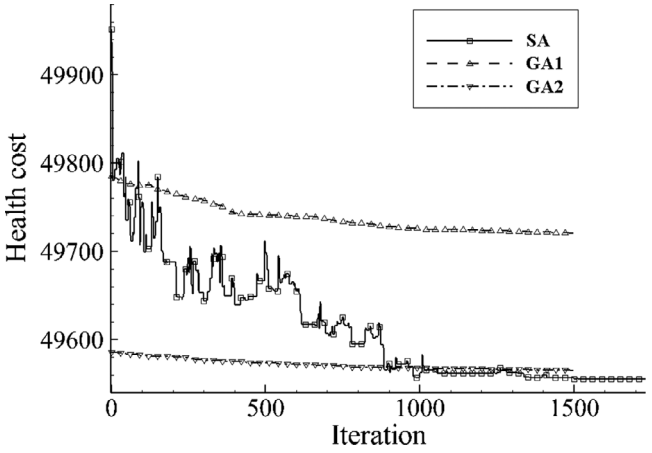

FIGURE 3 Convergence curve of the simulated annealing algorithm and genetic algorithms.

number of iterations, the SA algorithm has a lower health cost than GA1 and GA2. In addition, over 1500 iterations, these algorithms' computational times for a $35 \times 25 \times 50$ grid are 36 h, 60 h, and 57 h, respectively. Taken together, these results show that the SA algorithm has a high computational efficiency. Thus, the SA algorithm is used to solve our bilevel problem.

Furthermore, the convergence curve of the SA algorithm in Figure 3 shows that although there are initially some fluctuations in the value of the objective function, the overall trend is decreasing as the number of iterations increases (e.g., to 1000). As the number of iterations increases beyond 1000, the objective value stabilizes and the optimal solution is found. This result is consistent with the expectation of the SA and demonstrates the high probability of a minimized value being obtained. The additional housing allocation is assumed to be nonnegative (i.e., $h \geq 0$) in the constraint of the upper level subprogram (Equation 34), so the initial solution (i.e., $h = 0$) is a good choice. This confirms that the initial solution influences the number of iterations needed to achieve convergence. Figure 4 depicts a clear grid convergence and thus a $35 \times 25 \times 50$ grid is selected for further discussions.

The plot of the optimal additional housing allocation with a minimized health cost Y is shown in Figure 5. First, a positive relationship is observed between an additional housing allocation and the distance to the central CBD. In other words, the allocation of additional housing units increases as the distance from the CBD increases. This result can be explained by lower rents and better air quality in locations distant from the CBD, despite the high traffic-related cost. This study assumes that the air quality is an important determinant of the housing location. Therefore, more people will choose to live in a location far from the CBD despite a smaller utility function. As our object function is integrated by the product of the travel demand and air quality, this value will decrease as more people choose housing locations far from the CBD. Second, under our assumption, the additional housing allocation is also dependent on the direction of the CBD. Figure 5 demonstrates that the northeast region of the CBD has fewer allocated additional housing units than the southwest region. Possibly, more people already live in the region northeast of the CBD, and therefore this region will be more congested throughout the day. Apart from the high traffic-related cost, this region also has poorer air quality due to the eastward wind direction. Third, in contrast to Yin et al. (2013), who observed the highest additional housing allocation around the CBD, this study demonstrates the lowest allocation of additional housing units to be around the CBD because of the adoption of the health cost, a product of the air pollutant concentration and demand at a location, as the objective housing allocation problem (upper level subprogram). This leads to the allocation of housing units to locations with less air pollution (or traffic).

Under the optimal dynamic departure time principle, travelers may choose the best departure time to travel to or return from the CBD, such that their total travel cost is minimized. Figure 6 shows temporal variations in the travel demand and the total travel cost (6:00 a.m. to 6:00 a.m.$^{+1}$) incurred by travelers at different points within the modeling region when traveling to and from the CBD. Here, the peak travel demand always corresponds to the time when the total travel cost is lowest, thus satisfying the dynamic user-optimal condition principle. Therefore, all travelers will choose a departure time to minimize and equalize their total travel cost. As shown in each subfigure of Figure 6, the total travel cost decreases (or increases) linearly with time during the beginning (or ending) period, when the whole city is noncongested. Accordingly, the actual travel cost should be unchanging during this period. Therefore, changes in the total travel cost depend only on the schedule-delay cost (i.e., early- and late-arrival penalty), which has a linear relationship with the departure time with respect to the value of an early or late arrival time.

Figure 7 depicts the city-wide distribution of best departure times during the first period T^1 and that of the best arrival time during the second period T^2. Figure 7a shows that as the desired arrival time interval is [8:36 a.m., 9:00 a.m.], the departure time of all travelers is earlier than 8:36 a.m., and travelers who reside close to the CBD have later departure times. Figure 7b shows that the desired departure time interval from the CBD is [6:18 p.m., 6:42 p.m.]. Thus, all travelers arrive later than 6:42 p.m., and travelers who reside farther from the CBD have later arrival times.

Figure 8 shows the distributions of the density (ρ), travel cost (ϕ), and vehicle exhaust concentration (C) for

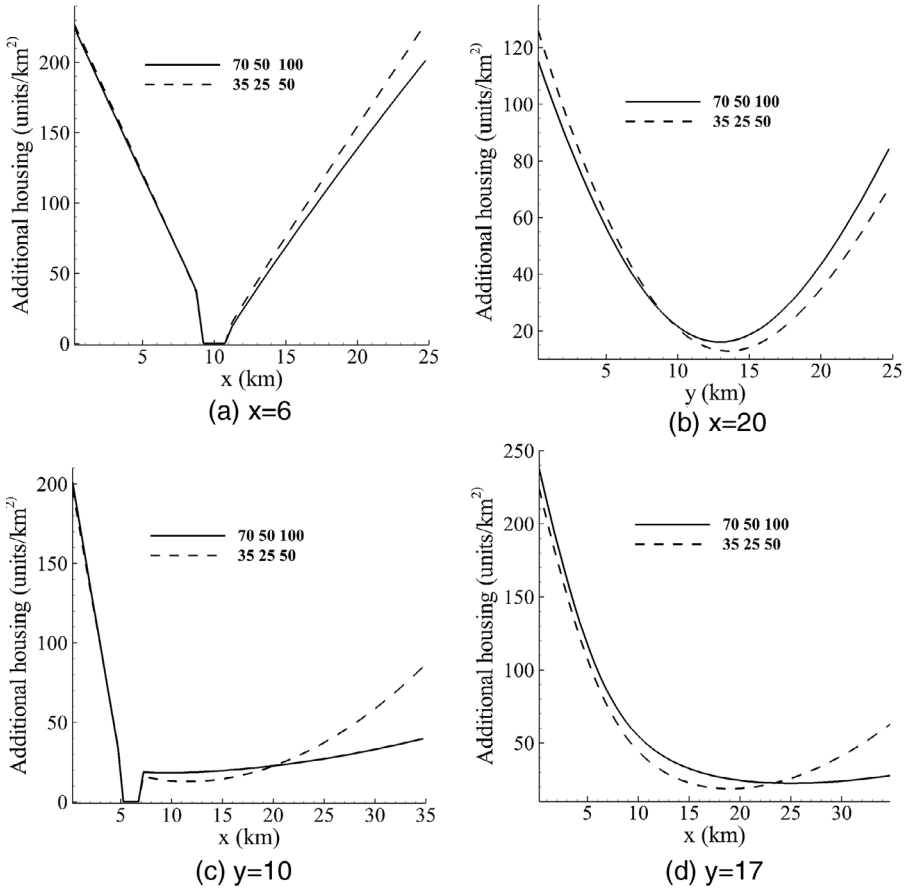

FIGURE 4 The grid convergence of additional housing allocation.

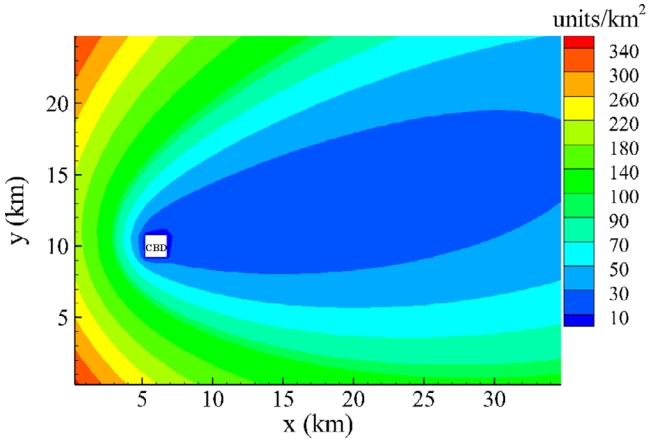

FIGURE 5 Distribution of the optimal additional housing allocation.

travelers traveling to the CBD. As shown in the left column, no travelers are in the city at 8:00 a.m., which is too early for travel to the CBD and would incur an early arrival penalty. At 8:24 a.m., all travelers are located in the eastern region because travelers who reside near the CBD have not yet departed, while those who reside further away and had departed earlier have arrived. At 8:48 a.m., all travelers are concentrated around the CBD, in other words, the travelers are approaching or have entered the CBD. At 9:12 a.m., all travelers have entered the CBD and left the transportation system. In the middle column, the travel cost contours at 8:00 and 9:12 a.m. appear as series of concentric circles about the CBD because the vehicle is rare (see the left column). At 8:24 and 8:48 a.m., the travel cost contours become denser (i.e., the local cost of a moving unit distance increases) because as the travelers gradually depart for the CBD, the density increases within the city and the travel cost increases accordingly. By comparing the distributions of the density and travel cost (i.e., the left and middle columns), high-density locations are shown to have denser travel cost contours. The right column depicts a positive relationship of the pollutant concentration with density. The influence of wind is demonstrated by a higher pollutant concentration in the downwind region (i.e., east of the CBD) than the upwind region.

Figure 9 shows the distributions of the density (ρ), travel cost (ϕ), and vehicle exhaust concentration (C) for the travelers returning from the CBD. In the left column, there are no travelers in the city at 6:00 p.m. At 6:24 and 6:36 p.m., the travelers then concentrate gradually around the CBD, especially the northeast region. This pattern is explained

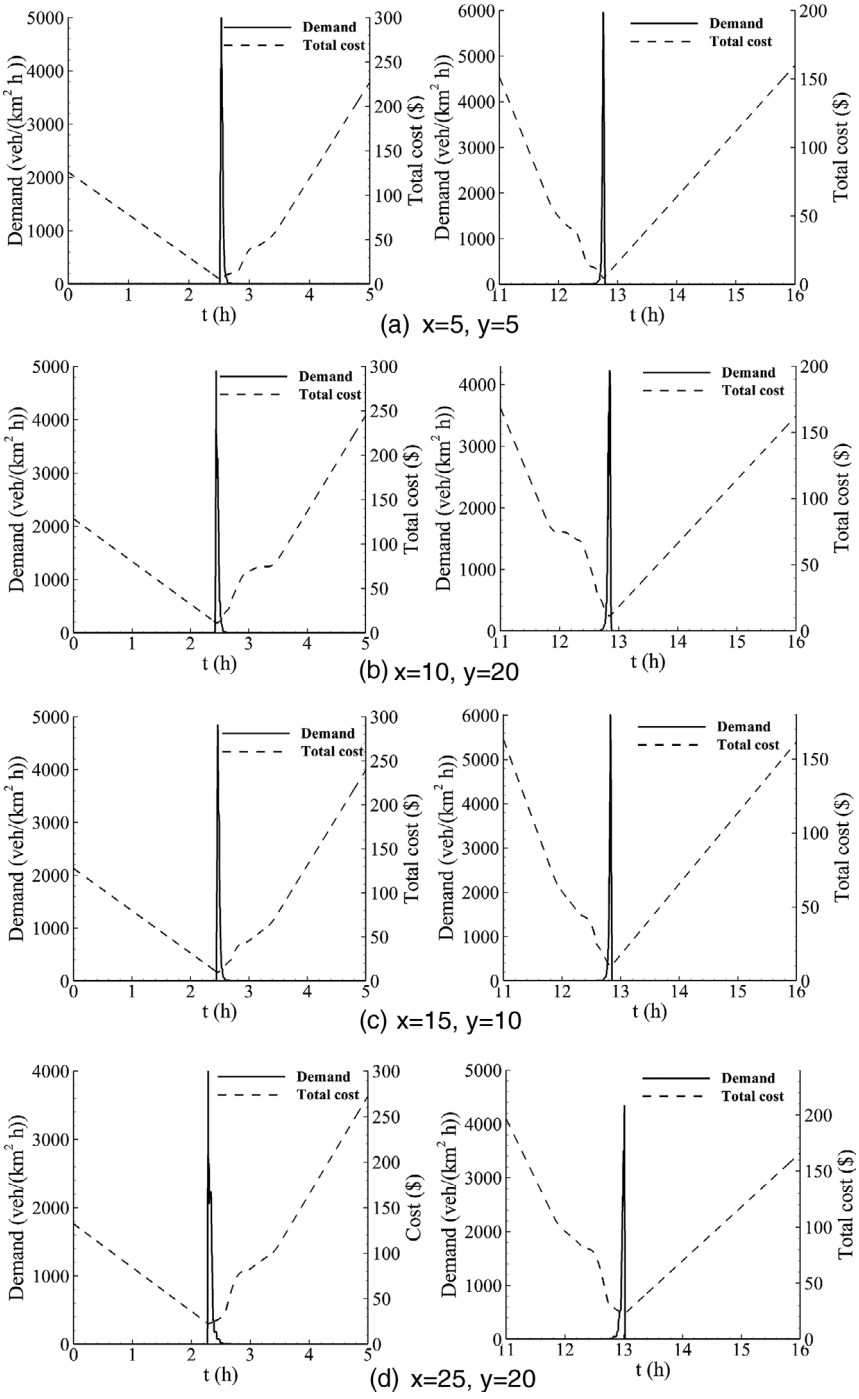

FIGURE 6 Analysis of travel demand and total travel cost. Left, vehicles traveling to the central business district (CBD); right, vehicles traveling back from the CBD.

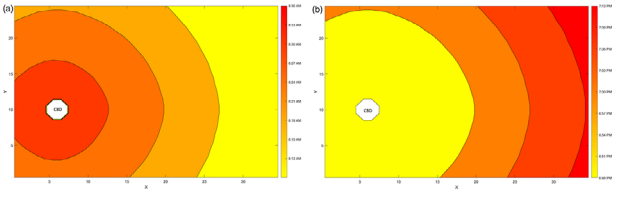

FIGURE 7 Distribution of the (a) best departure times for a traveler traveling to the central business district (CBD) and (b) best arrival times for returning from the CBD.

by the travelers' desired departure period of 6:18 to 6:42 p.m. In this period, travelers leave the CBD gradually, resulting in a high density around this region. At 6:48 p.m., this high-density region moves away from the CBD because the travelers who reside far away from the CBD have not yet arrived at home. In the middle column, the travel cost contours at 6:00 and 6:48 p.m. are series of concentric circles because the vehicle is rare (see the left column). At 6:24 and 6:36 p.m., the travel cost contours become denser (i.e., the local cost of moving a unit distance increases) because the density increases within the

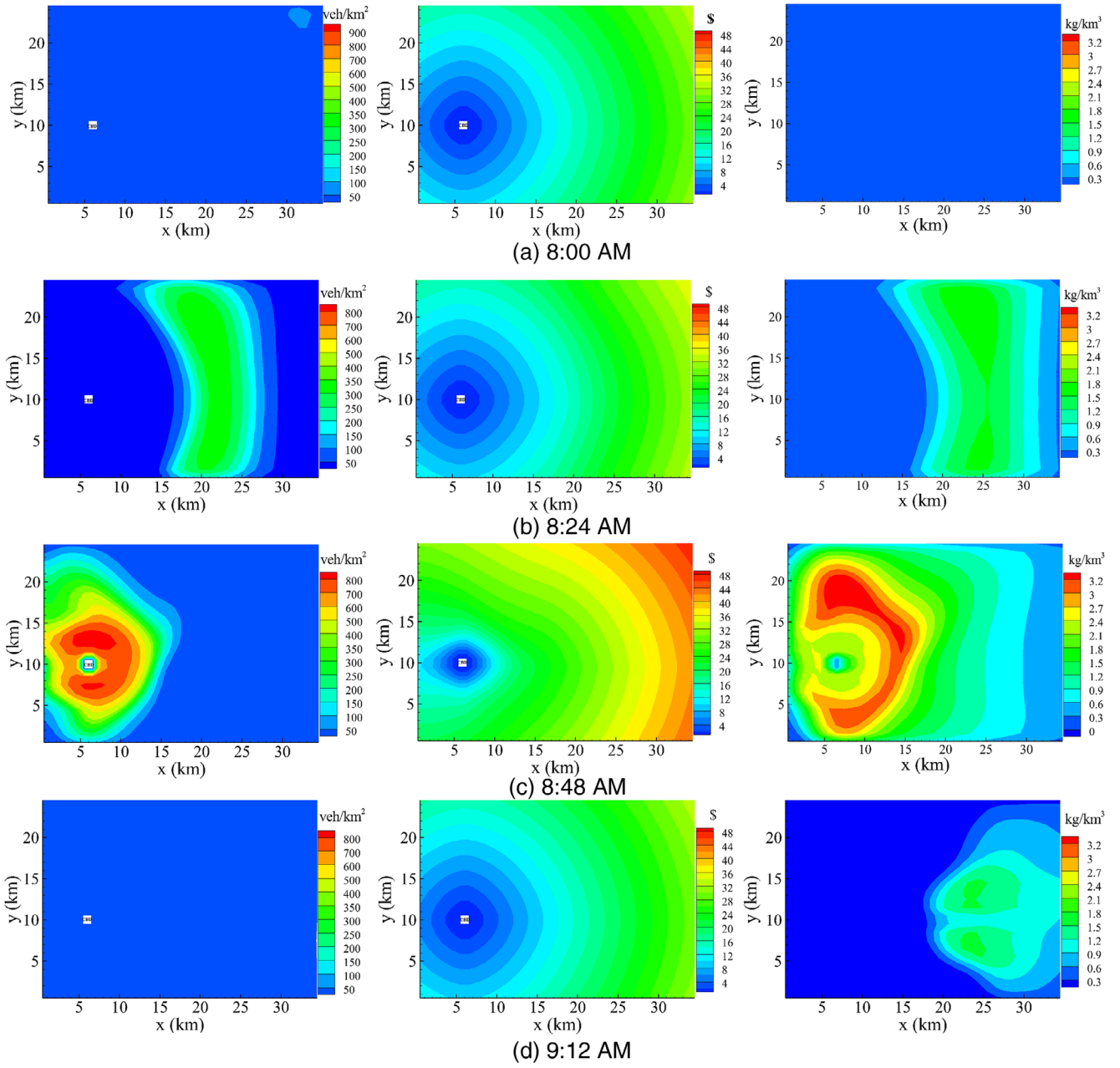

FIGURE 8 Distributions of density (left column in veh/km^2), travel cost (right column in \$), and pollutant concentration (right column in kg/km^3) corresponding to travel to the central business district (CBD).

travel cost increases. By comparing the distributions of density and travel cost (i.e., the left and middle columns), high-density locations are shown to have denser travel cost contours. In the right column, the pollutant concentration is shown to be positively associated with density. The downwind region (i.e., east of the CBD) is more polluted than the upwind region because of the influence of wind.

The actual traffic flow over the whole modeling region at different times is considered, defined as

$$F(t) = \int_{\Omega} \rho(x, y, t)\, dxdy \tag{40}$$

Figure 10 shows the plot of total traffic flow over the whole area versus time t. In the first period (6:00 a.m. ~ 5:00 p.m.), the total traffic flow accumulates quickly from 8:00 a.m. and reaches a peak at 8:36 a.m. After 8:36 a.m., the total flow decreases as travelers gradually enter the CBD. Eventually, as all travelers enter the CBD, the total traffic flow equals zero. The total traffic flow for the second period (5:00 p.m. ~ 6:00^{+1} a.m.) is similar to that in the first period but in reverse.

Figure 11 depicts the distributions of the average travel cost, housing rent, and average pollutant concentration. In Figure 11a, the average travel cost increases with the

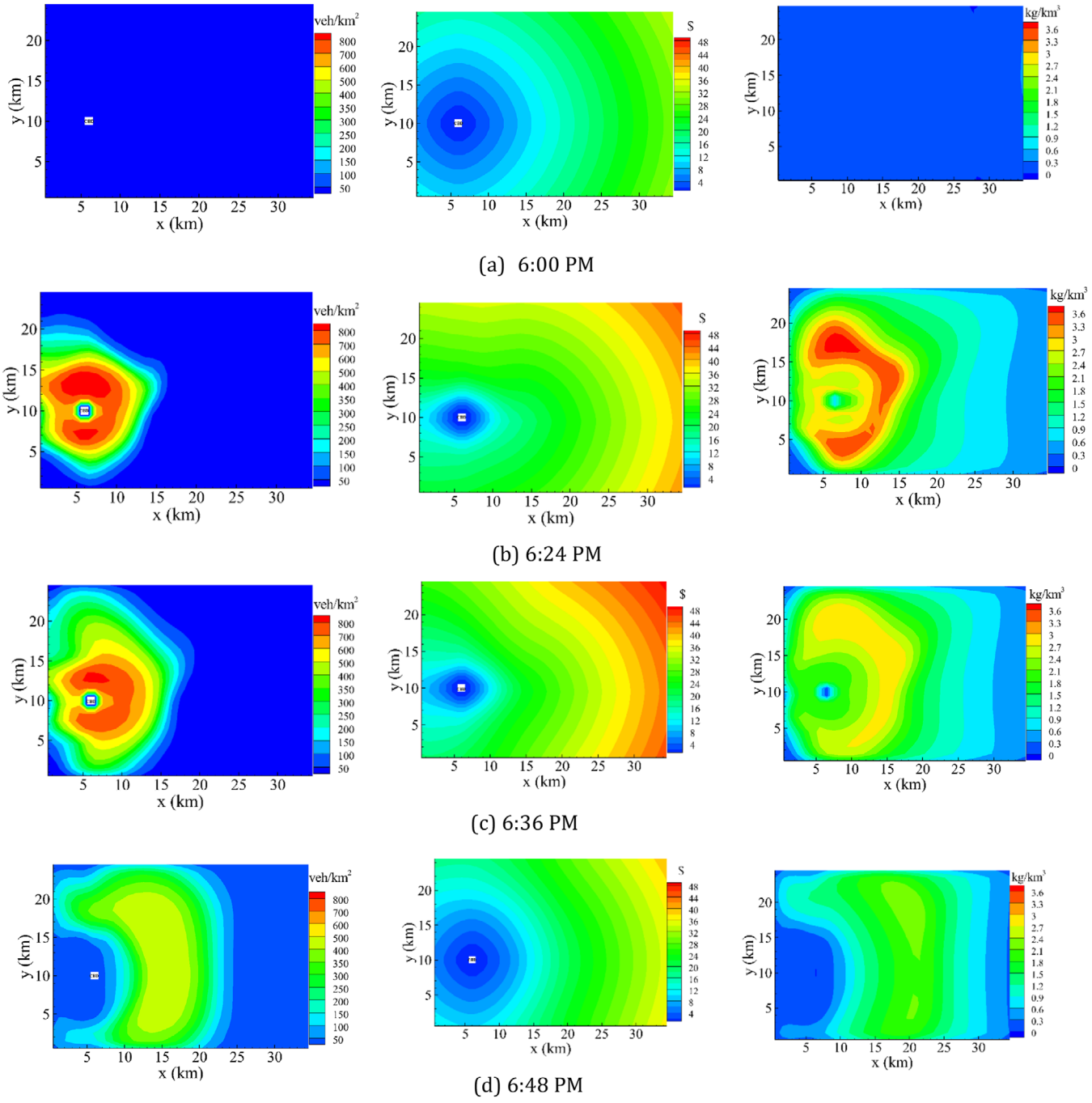

FIGURE 9 Distributions of density (left column in veh/km^2), travel cost (right column in \$), and pollutant concentration (right column in kg/km^3) corresponding to the return from the central business district (CBD).

distance to the CBD. This cost is lower in the southwest region than in the northeast region. The travel cost is lower in the southwest region due to the shorter travel distance and because the increase in cost is slower (as indicated by more sparse contour lines) in the southwest region than in the northeast region due to the reduced traffic from the west (there is less congestion). In Figure 11b, the housing rent decreases with the distance to the CBD. Housing rent is very high in the region near the CBD because of the limited housing provision and high travel demand (and low travel-related cost). In Figure 11c, the downwind region is much more polluted than the upwind region. Particularly, the northeast region is highly polluted because of the heavy traffic and higher number of travelers who live in this region.

Figure 12a, b show that when moving from the CBD to the outer boundary of the city, the travel demand increases with the distance to CBD to a maximum value, after

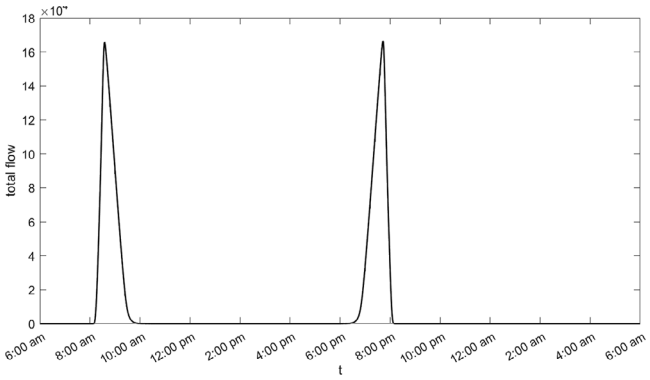

FIGURE 10 Total traffic flow across the whole modeling region.

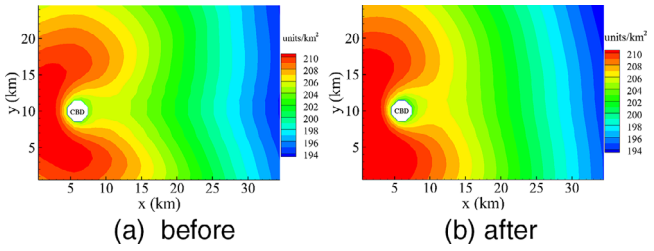

FIGURE 12 The distribution of the travel demand before and after the additional housing allocation.

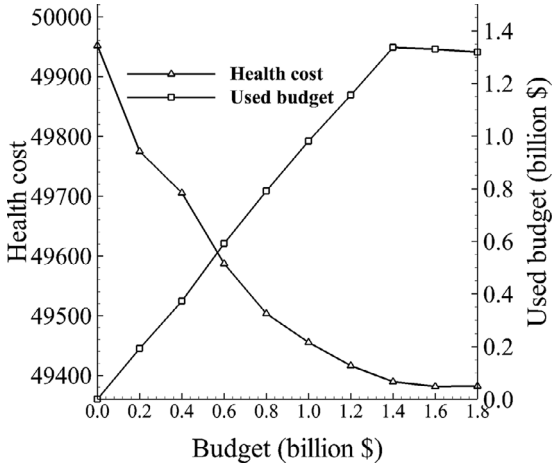

FIGURE 13 Sensitivity of the health cost to budget *B*.

which the travel demand decreases with increasing distance to the CBD. This result can be explained by the nature of a traveler's housing location choice as a trade-off between the travel-related cost, housing rent, and air quality. Regions far from the CBD have low housing rents and good air quality, but high travel-related costs. In contrast, regions close to the CBD have low travel-related costs, but poor air quality and extremely high housing rents. Under these three factors, the travel demand will reach a peak at a certain distance from the CBD. A further comparison of Figure 12a and b reveals that the travel demands west of the CBD increase because most of the allocated housing is added in that region.

Figure 13 demonstrates the sensitivity of the health cost (Y) with respect to the available budget (B). In general, the health cost Y decreases as the budget increases because the latter enables the provision of more housing units. Therefore, an additional housing pattern that would attract travelers to reside in certain locations or would further reduce the health cost could enable greater flexibility. However, the health cost is more sensitive to a budget increase when the budget is small (e.g., \$0.2 ~ 0.6 billion), but is less sensitive when the budget exceeds \$1.4 billion. Figure 13 shows that the budgeted funds are used when the total budget is less than \$1.4 billion, whereas a surplus occurs with larger budgets. In other words, an increase in investment can effectively decrease the health cost to a certain point (up to \$1.4 billion in this case). Planners must determine this point during the planning process.

Figure 14 demonstrates the sensitivity of the health cost (Y) with respect to the maximum additional housing supply $h_{\max}$. In general, the health cost Y decreases as the maximum additional housing supply increases because the latter enables the provision of more housing units at the same location. Thus, the provision of an additional

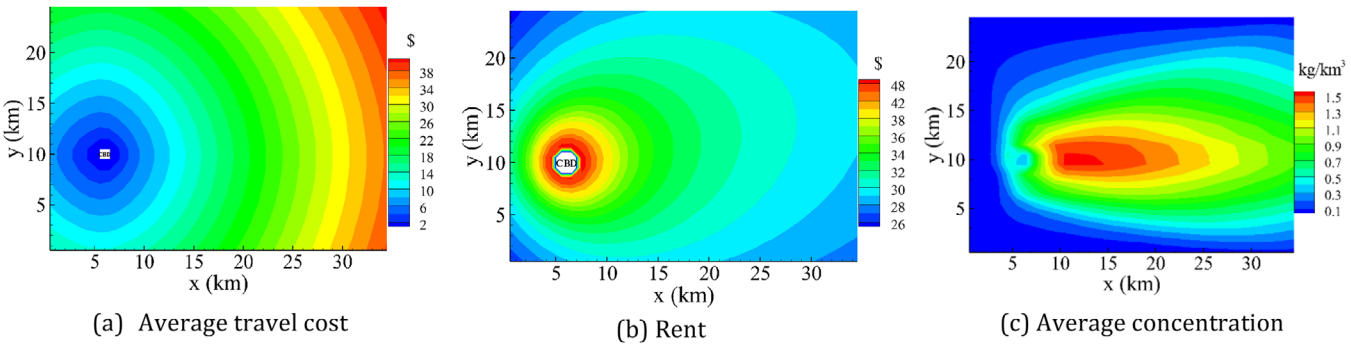

FIGURE 11 The determining factors of housing location. (a) Travel cost distribution (\$); (b) housing rent distribution (\$); (c) average pollutant concentration (kg/km^3).

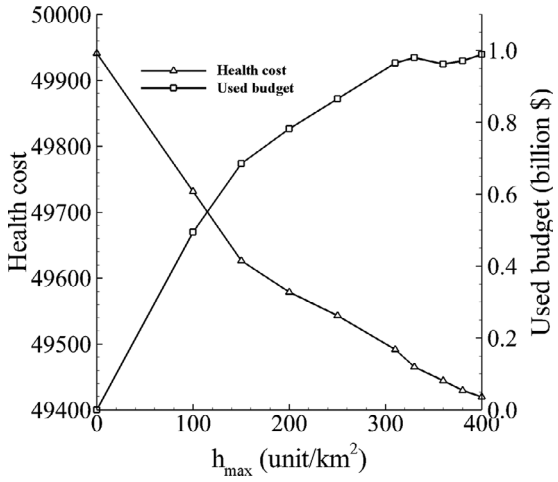

FIGURE 14 Sensitivity of the health cost to the maximum additional housing supply, h_{max}.

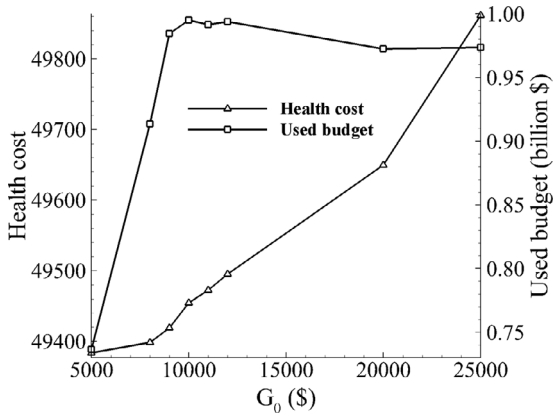

FIGURE 15 Sensitivity of the health cost to the basic supply cost, G_0.

housing pattern to reduce the health cost would provide more flexibility. However, the health cost is more sensitive to an increase in an initially small maximum additional housing supply (e.g., $0 \sim 150$ unit/km^2), but becomes less sensitive when the maximum additional housing supply exceeds 320 unit/km^2. Figure 14 also demonstrates a budget surplus when the maximum additional housing supply is less than 320 unit/km^2, whereas all funds are used when the maximum additional housing supply exceeds 320 unit/km^2. Accordingly, an increase in the maximum additional housing supply is also a valid way to reduce the health cost to a certain point (e.g., up to 320 unit/km^2 in this case, with budgetary limitations). Thus, it is important to determine the link between the health cost and maximum additional housing supply in land use.

Figure 15 shows the sensitivity of the health cost (Y) to the basic supply cost, G_0. Here, the health cost, Y, increases as the basic supply cost increases. Consequently, the supply cost, G, will also increase, thus reducing the number of provided housing units. Ultimately, it would be more difficult to provide an additional housing pattern that would attract travelers to reside in locations that could further increase the health cost. However, the health cost is more sensitive to an increase in the budget when the basic supply cost is high (e.g., \$15000–25000), but becomes less sensitive when the basic supply costs less than \$10,000. As shown in Figure 15, all budgeted funds are used when the basic supply cost exceeds \$10,000, whereas a surplus remains when the budget is less than \$10,000. In other words, reducing the basic cost or increasing the budget are effective ways to decrease the health cost. Planners must determine this value during the planning process.

Figure 16 shows the distribution of the travel demand at different values of ξ, a measure of the sensitivity of travelers to the concentration of pollutants with respect to the housing utility function (see Equations 28 and 29). As ξ increases, the influence of the air quality on the choice of housing location becomes stronger. In Figure 16a, when $\xi = 0$, the housing allocation only depends on the rent and travel cost, and therefore the contours form concentric circles around the center of the CBD. In contrast, ξ is not zero in Figure 16b and c, and the travel demands are influenced by the air quality. For example, the travel demands are lower in locations downwind of the CBD (i.e., east side) because the pollutants emitted around the CBD are dispersed by wind in this direction.

5 | CONCLUSION

In this study, a bilevel model was proposed to study a housing allocation problem while considering traffic-related

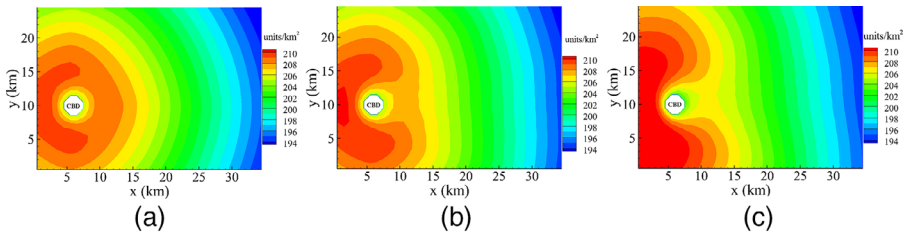

FIGURE 16 Distribution of the travel demand at different values of ξ.

emissions in a dynamic continuum transportation system. For the lower level, the PDUO-C model with a combined departure time and route choice was adopted to model the traffic flows and the travelers' housing location choice, which depends on the traffic-related cost, housing rent, and air quality, for a given housing allocation. The lower level subprogram was formulated as a fixed-point problem, a Lax–Friedrichs scheme and fast-sweeping method are used as the solution algorithm. At the upper level, the health cost, which depends on the concentration of pollutants and the number of residents, was minimized by optimizing the housing additional allocation pattern. An SA algorithm was adopted to solve this optimization problem. A numerical example was then completed to demonstrate the effect of consideration of the health cost in the optimal design of the housing allocation. Sensitivity analyses were also conducted to demonstrate the influences of various factors (e.g., budget, cost of housing supply) on the optimized health cost and travel demand pattern.

This study considered only a unidirectional wind. In reality, however, a multidirectional wind is more common and should be considered in a future study. In this study, an SA algorithm, a nature-inspired optimization algorithm, is adopted to solve the upper level subprogram. This algorithm has enormous computational time and cost requirements for solving the devised bilevel housing allocation problem. Therefore, to ensure that the upper level subprogram can be solved in a fast and effective manner, other advanced nature-inspired optimization algorithms and related techniques—such as the harmony search algorithm (Siddique & Adeli, 2015), water drop algorithms (Siddique & Adeli, 2014), the gravitational search algorithm (Siddique & Adeli, 2016), the bacteria foraging algorithm (Wang et al., 2018), spider monkey optimization (Akhand et al., 2020), and meta-heuristic multi- and many-objective optimization techniques (Rodrigues et al., 2017)—will be considered and evaluated in future research. In this paper, only trips from travelers' home locations to the CBD or from the CBD back to their home locations are considered. Other trips (e.g., trips between the home locations of different travelers) are ignored. In future studies, asymmetric and overlapping demand will be investigated.

ACKNOWLEDGMENTS

The study described in this paper was supported by grants from the Research Grants Council of the Hong Kong Special Administrative Region, China (Project No. 17208614), and Guangdong–Hong Kong–Macau Joint Laboratory Program of the 2020 Guangdong New Innovative Strategic Research Fund, Guangdong Science and Technology Department (Project No.: 2020B1212030009). The second author was also supported by the Francis S Y Bong Professorship in Engineering. The fourth author is supported by NSF grant DMS-2010107. The fifth author was supported by NSFC Grant 11471305.

REFERENCES

Ahn, K., Trani, A., Rakha, H., & VanAerde, M. (1999). Microscopic fuel consumption and emission models. In *Proceedings of the 78th annual meeting of the transportation research board*. Washington, DC, USA.

Akhand, M. A. H., Ayon, S. I., Shahriyar, S. A., Siddique, N., & Adeli, H. (2020). Discrete spider monkey optimization for travelling salesman problem. *Applied Soft Computing*, *86*, 105887.

Barthelemy, M. (2016). *The structure and dynamics of cities*. Cambridge University Press.

Bell, M., Cassir, C., Iida, Y., & Lam, W. (1999). A sensitivity-based approach to network reliability assessment. In *Proceedings of the 14th international symposium on transportation and traffic theory* (pp. 283–300).

Ben-Akiva, M., & Bowman, J. L. (1998). Integration of an activity-based model system and a residential location model. *Urban Studies*, *35*(7), 1131–1153.

Bhat, C R., & Guo, J. (2004). A mixed spatially correlated logit model: Formulation and application to residential choice modeling. *Transportation Research Part B: Methodological*, *38*(2), 147–168.

Blumenfeld, D. E. (1977). Modeling the joint distribution of home and workplace locations in a city. *Transportation Science*, *11*(4), 307–337.

Boyce, D., & Mattsson, L.-G. (1999). Modeling residential location choice in relation to housing location and road tolls on congested urban highway networks. *Transportation Research Part B: Methodological*, *33*(8), 581–591.

Britter, R. E., & Hanna, S. R. (2003). Flow and dispersion in urban areas. *Annual Review of Fluid Mechanics*, *35*(1), 469–496.

CARB. (2006). Emfac2007 version 2.30 user guide: Calculating emission inventories for vehicles in California *(Tech. Rep.)*. California Air Resource Board.

Chang, J. S., & Mackett, R. L. (2006). A bi-level model of the relationship between transport and residential location. *Transportation Research Part B: Methodological*, *40*(2), 123–146.

Chen, M., & Liu, Y. (2010). NO*x* removal from vehicle emissions by functionality surface of asphalt road. *Journal of Hazardous Materials*, *174*(1-3), 375–379.

Du, J., Wong, S. C., Shu, C.-W., Xiong, T., Zhang, M., & Choi, K. (2013). Revisiting Jiang's dynamic continuum model for urban cities. *Transportation Research Part B: Methodological*, *56*, 96–119.

Echenique, M. H. (1985). *The use of integrated land use transportation planning models: The cases of Sao Paulo*. Elsevier.

Ellickson, B. (1981). An alternative test of the hedonic theory of housing markets. *Journal of Urban Economics*, *9*(1), 56–79.

Environmental-Protection-Agency. (1994). *User's guide to mobile5: (Mobile source emission factor model)*. US Environmental Protection Agency, Office of Mobile Sources. Emission Planning and Strategies Division.

Ermak, D. L. (1977). An analytical model for air pollutant transport and deposition from a point source. *Atmospheric Environment (1967)*, *11*(3), 231–237.

Fallah-Shorshani, M., Shekarrizfard, M., & Hatzopoulou, M. (2017). Integrating a street-canyon model with a regional Gaussian

dispersion model for improved characterisation of near-road air pollution. *Atmospheric Environment*, *153*, 21–31.

Giuliano, G. (1989). Research policy and review 27. New directions for understanding transportation and land use. *Environment and Planning A*, *21*(2), 145–159.

Hansen, W. G. (1959). How accessibility shapes land use. *Journal of the American Institute of Planners*, *25*(2), 73–76.

Hargreaves, D. M., & Baker, C. J. (1997). Gaussian puff model of an urban street canyon. *Journal of Wind Engineering and Industrial Aerodynamics*, *69*, 927–939.

Hartwick, P. G., & Hartwick, J. M. (1974). Efficient resource allocation in a multinucleated city with intermediate goods. *The Quarterly Journal of Economics*, *88*(2), 340–352.

Hickman, A., & Colwill, D. (1982). The estimation of air pollution concentration from road traffic *(Tech. Rep. No. TRRL Supplementary Report No.1052)*. Transport and Road Research Laboratory Assessment Division, Transport System Department.

Ho, H. W., & Wong, S. C. (2007). Housing allocation problem in a continuum transportation system. *Transportmetrica*, *3*(1), 21–39.

Ho, H. W., Wong, S. C., & Loo, B. P. Y. (2006). Combined distribution and assignment model for a continuum traffic equilibrium problem with multiple user classes. *Transportation Research Part B: Methodological*, *40*(8), 633–650.

Hunt, J. D., & Abraham, J. E. (2005). Design and implementation of PECAS: A generalised system for allocating economic production, exchange and consumption quantities. In *Integrated land-use and transportation models* (pp. 253–273). Emerald Group Publishing Limited.

International-Energy-Agency. (2006). CO_2 emissions from fuel combustion 1971–2004 *(Tech. Rep.)*. International Energy Agency.

Kirkpatrick, S., Gelatt, C. D., & Vecchi, M. P. (1983). Optimization by simulated annealing. *Science*, *220*(4598), 671–680.

Labbé, M., Marcotte, P., & Savard, G. (1998). A bilevel model of taxation and its application to optimal highway pricing. *Management Science*, *44*(12-part-1), 1608–1622.

Lee, D.-H., & Boyce, D. E. (2004). *Urban and regional transportation modeling: Essays in honor of David Boyce*. Edward Elgar Publishing.

Lin, Z. Y., Wong, S. C., Zhang, P., & Zhang, X. N. (2021). Bilevel dynamic continuum model for housing allocation and transportation emission problems in an urban city. *International Journal of Sustainable Transportation*, *15*(1), 55–69.

Loos, C., Seppelt, R., Meier-Bethke, S., Schiemann, J., & Richter, O. (2003). Spatially explicit modelling of transgenic maize pollen dispersal and cross-pollination. *Journal of Theoretical Biology*, *225*(2), 241–255.

Lowry, I. S. (1964). A model of metropolis *(Tech. Rep.)*. Rand Corporation.

Metropolis, N., Rosenbluth, A. W., Rosenbluth, M. N., Teller, A. H., & Teller, E. (1953). Equation of state calculations by fast computing machines. *The Journal of Chemical Physics*, *21*(6), 1087–1092.

Nagurney, A., Qiang, Q., & Nagurney, L. S. (2010). Environmental impact assessment of transportation networks with degradable links in an era of climate change. *International Journal of Sustainable Transportation*, *4*(3), 154–171.

Nagurney, A., Ramanujam, P., & Dhanda, K. K. (1998). A multimodal traffic network equilibrium model with emission pollution permits: Compliance vs noncompliance. *Transportation Research Part D: Transport and Environment*, *3*(5), 349–374.

Nejadkoorki, F., Nicholson, K., Lake, I., & Davies, T. (2008). An approach for modelling CO_2 emissions from road traffic in urban areas. *Science of the Total Environment*, *406*(1-2), 269–278.

Nizich, S. V., Misenheimer, D., Pierce, T., Pope, A., & Carlson, P. (1994). National air pollutant emissions trends, 1900–1993 *(Tech. Rep.)*. Office of Air Quality Planning and Standards.

Ogawa, H., & Fujita, M. (1980). Equilibrium land use patterns in a non-monocentric city. *Journal of Regional Science*, *20*(4), 455–475.

Qi, J., Wang, S., & Psaraftis, H. (2021). Bi-level optimization model applications in managing air emissions from ships: A review. *Communications in Transportation Research*, *1*, 00020.

Rodrigue, J.-P., Comtois, C., & Slack, B. (2016). *The geography of transport systems*. Routledge.

Rodrigues, D., Papa, J. P., & Adeli, H. (2017). Meta-heuristic multi-and many-objective optimization techniques for solution of machine learning problems. *Expert Systems*, *34*(6), e12255.

Rosen, S. (1974). Hedonic prices and implicit markets: Product differentiation in pure competition. *Journal of Political Economy*, *82*(1), 34–55.

Schirmer, P. M., Van Eggermond, M. A. B., & Axhausen, K. W. (2014). The role of location in residential location choice models: A review of literature. *The Journal of Transport and Land Use*, *7*(2), 3–21.

Small, K. A. (1982). The scheduling of consumer activities: Work trips. *The American Economic Review*, *72*(3), 467–479.

Smit, R., Smokers, R., & Rabé, E. (2007). A new modelling approach for road traffic emissions: Versit+. *Transportation Research Part D: Transport and Environment*, *12*(6), 414–422.

Siddique, N., & Adeli, H. (2014). Water drop algorithms. *International Journal on Artificial Intelligence Tools*, *23*(06), 1430002.

Siddique, N., & Adeli, H. (2015). Harmony search algorithm and its variants. *International Journal of Pattern Recognition and Artificial Intelligence*, *29*(08), 1539001.

Siddique, N., & Adeli, H. (2016). Gravitational search algorithm and its variants. *International Journal of Pattern Recognition and Artificial Intelligence*, *30*(08), 1639001.

Soffer, L., Burson, S., Ferrell, C., Lee, R., & Ridgely, J. (1995). *Accident source terms for light-water nuclear power plants*. Final report (Tech. Rep. No. NUREG-1465. Nuclear). Nuclear Regulatory Commission.

Stockie, J. M. (2011). The mathematics of atmospheric dispersion modeling. *SIAM Review*, *53*(2), 349–372.

Tong, H., Hung, W., & Cheung, C. S. (2000). On-road motor vehicle emissions and fuel consumption in urban driving conditions. *Journal of the Air & Waste Management Association*, *50*(4), 543–554.

Turner, R., & Hurst, T. (2001). Factors influencing volcanic ash dispersal from the 1995 and 1996 eruptions of Mount Ruapehu, New Zealand. *Journal of Applied Meteorology*, *40*(1), 56–69.

Vallamsundar, S., & Lin, J. J. (2011). Moves versus mobile:Comparison of greenhouse gas and criterion pollutant emissions. *Transportation Research Record*, *2233*(1), 27–35.

Vaughan, R. (1987). *Urban spatial traffic patterns*. Pion.

Waddell, P. (1998). An urban simulation model for integrated policy analysis and planning: Residential location and housing market components of urbansim.

Wagner, P., & Wegener, M. (2007). Urban land use, transport, and environment models. Experiences with an integrated microscopic approach. *DisP-The Planning Review*, *43*(170), 45–56.

Wang, J., Zhong, D., Adeli, H., Wang, D., & Liu, M. (2018). Smart bacteria-foraging algorithm-based customized kernel support vector regression and enhanced probabilistic neural network for compaction quality assessment and control of earth-rock dam. *Expert Systems*, *35*(6), e12357.

Wardrop, J. G. (1952). Road paper. Some theoretical aspects of road traffic research. *Proceedings of the Institution of Civil Engineers*, *1*(3), 325–362.

Wegener, M. (2004). Overview of land use transport models. In *Handbook of transport geography and spatial systems* (pp. 127–146). Emerald Group Publishing Limited.

Wheaton, W. C. (1977). Income and urban residence: An analysis of consumer demand for location. *The American Economic Review*, *67*(4), 620–631.

Yang, L., Li, T., Wong, S. C., Shu, C.-W., & Zhang, M. (2019). Modeling and simulation of urban air pollution from the dispersion of vehicle exhaust: A continuum modeling approach. *International Journal of Sustainable Transportation*, *13*(10), 722–740.

Yang, L., Wong, S. C., Ho, H. W., Zhang, M., & Shu, C.-W. (2022). Effects of air quality on housing location: A predictive dynamic continuum user-optimal approach. *Transportation Science*, *56*(5), 1111–1134.

Yin, J., Wong, S. C., Choi, K., & Du, Y. C. (2017). A continuum modeling approach to the spatial analysis of air quality and housing location choice. *International Journal of Sustainable Transportation*, *11*(5), 319–329.

Yin, J., Wong, S. C., Sze, N. N., & Ho, H. W. (2013). A continuum model for housing allocation and transportation emission problems in a polycentric city. *International Journal of Sustainable Transportation*, *7*(4), 275–298.

Yin, Y., & Lawphongpanich, S. (2006). Internalizing emission externality on road networks. *Transportation Research Part D: Transport and Environment*, *11*(4), 292–301.

Zondag, B., & Pieters, M. (2005). Influence of accessibility on residential location choice. *Transportation Research Record*, *1902*(1), 63–70.

How to cite this article: Yang, L., Wong, S. C., Ho, H. W., Shu, C.-W., & Zhang, M. (2023). Bilevel optimization of a housing allocation and traffic emission problem in a predictive dynamic continuum transportation system. *Computer-Aided Civil and Infrastructure Engineering*, *38,* 2576–2596. https://doi.org/10.1111/mice.13007